THE JOURNAL OF BIOLOGICAL CHEMISTRY VOL. 288, NO. 5, pp. 3439–3448, February 1, 2013

ATP Alone Triggers the Outward Facing Conformation of the Maltose ATP-binding Cassette Transporter*

Received for publication, October 29, 2012, and in revised form, December 13, 2012 Published, JBC Papers in Press, December 14, 2012, DOI 10.1074/jbc.M112.431932

Huan Bao[1] **and Franck Duong**[2]

From the Department of Biochemistry & Molecular Biology, Life Sciences Institute, Faculty of Medicine, University of British Columbia, Vancouver, British Columbia V6T 1Z3, Canada

Background: The conformational cycle of $MalFGK_2$ is stimulated by ATP, MalE, and maltose.
Results: The transporter outward facing conformation depends on ATP only.
Conclusion: MalE and maltose must therefore stimulate the return of the transporter to the inward facing state.
Significance: Understanding the dynamics of the transporter is important to interpret the crystal structures.

The maltose transporter $MalFGK_2$ is a study prototype for ABC importers. During catalysis, the MalFG membrane domain alternates between inward and outward facing conformations when the MalK dimer closes and hydrolyzes ATP. Because a rapid ATP hydrolysis depends on MalE and maltose, it has been proposed that closed liganded MalE facilitates the transition to the outward facing conformation. Here we find that, in contrast to the expected, ATP is sufficient for the closure of MalK and for the conversion of MalFG to the outward facing state. The outward facing transporter binds MalE with nanomolar affinity, yet neither MalE nor maltose is necessary or facilitates the transition. Thus, the rapid hydrolysis of ATP observed in the presence of MalE and maltose is not because closed liganded MalE accelerates the formation of the outward facing conformation. These findings have fundamental implications for the description of the transport reaction.

ATP-binding cassette (ABC)[3] transporters are found both in prokaryotes and eukaryotes and transport a wide variety of substrates in and out of cells. The understanding of their mode of operation is relevant for medically important processes such as multidrug resistance, chloride conductance, cholesterol transport, and surface-antigen presentation (1). In bacteria, the maltose transporter has been studied for several decades as the prototype of ABC importers (2–4). The transporter is comprised of a cytosolic homodimeric ABC domain MalK bound to a membrane domain heterodimer, MalFG. On its periplasmic side, the transporter associates with the substrate-binding protein MalE that acts as a receptor for maltose.

Major progress in the description of ABC transporters has been achieved by x-ray crystallography (5–7). In the structure of $MalFGK_2$ without ligands, the sites for ATP binding on the MalK dimer are separated, and the MalFG membrane domain forms a cavity that is exposed to the cytosol (inward facing state) (8). In the structure obtained in the presence of MalE and nonhydrolyzable ATP analogs, the ATP-binding sites are bound together, whereas the MalFG cavity opens toward the periplasm (outward facing state) (6, 9). Together, these snapshots of the transporter structure have provided the molecular framework to explain how ATP binding and hydrolysis is coupled to membrane transport, the so-called alternating access mechanism. However, what triggers the transport reaction, why MalE stimulates ATP hydrolysis even in the absence of maltose, and how maltose is transferred from MalE to MalFG remain unclear.

MalE consists of two lobes with the maltose-binding site located at the interface. When the sugar binds, the two lobes close and eventually capture maltose with a high affinity (conformation termed closed liganded MalE) (10, 11). Because the ATPase activity of the transporter is maximal only in the presence of MalE and maltose, it has been proposed that closed liganded MalE binds the transporter and triggers ATP hydrolysis (12, 13). The x-ray structures were interpreted with this assumption in mind, leading to the model in Fig. 1*A* (2). In that model, the binding of closed liganded MalE to the transporter induces the pairing of MalK. The pairing of MalK triggers the MalFG outward facing conformation, which in turn forces the opening of MalE and the release of maltose. Upon ATP hydrolysis, the transporter returns to the inward facing state, and maltose enters the cytosol. In support of the model, an EPR spectroscopy study reported that the MalK nucleotide-binding interface closes only in the presence of MalE and ATP (14). A partial closure of the MalK interface was also observed when $MalFGK_2$ was co-crystallized with closed liganded MalE. It was concluded that MalE facilitates the pairing of MalK and therefore hydrolysis of ATP (15). However, despite the evidence and the prevalence of the model, we recently reported that closed liganded MalE does not bind the transporter but dissociates when MalE captures maltose. We also reported that open state MalE binds with nanomolar affinity to the outward facing transporter and creates a low affinity receptor for maltose (16). These data, difficult to reconciliate with the former model, led

* This work was supported by an infrastructure grant from the Canadian Foundation for Innovation.
[1] Supported by a Four Year Fellowship (FYF) from the University of British Columbia.
[2] Supported by Chaires de Recherche du Canada. To whom correspondence should be addressed: Dept. of Biochemistry & Molecular Biology, Life Sciences Institute, Faculty of Medicine, University of British Columbia, 2350 Health Sciences Mall, Vancouver, BC V6T 1Z3, Canada. Tel.: 604-822-5975; Fax: 604-822-522; E-mail: fduong@mail.ubc.ca.
[3] The abbreviations used are: ABC, ATP-binding cassette; DDM, *n*-dodecyl-β-D-maltoside; BMOE, bis-maleimidoethane; 5-IAF, 5-iodoacetamide fluorescein.

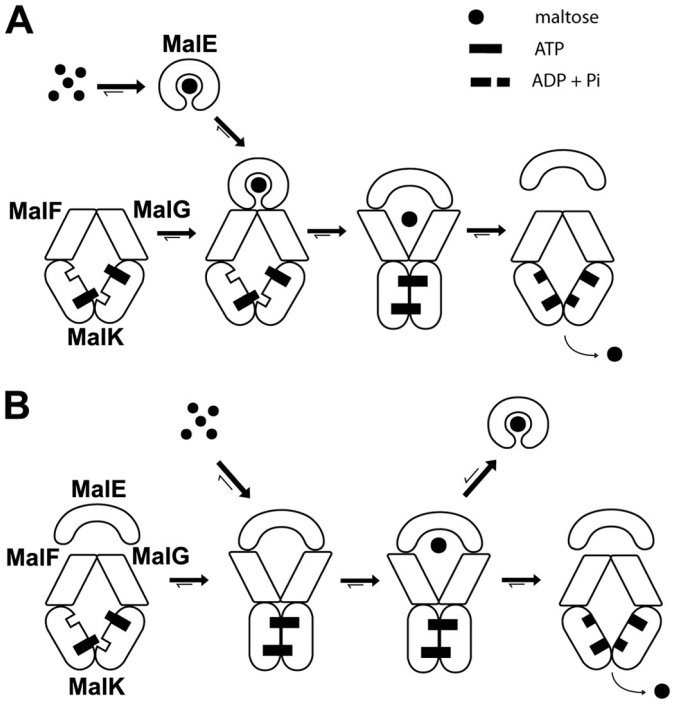

FIGURE 1. **Two opposed models for maltose transport.** *A*, in the conventional model, closed liganded MalE triggers the outward facing conformation. MalE binds maltose (K_d = ~2 μM) and then associates with the inward facing transporter (K_d > ~45 μM). The transition to the outward facing conformation facilitates the opening of MalE and the release of maltose to the MalFG cavity. Upon ATP hydrolysis, the transporter returns to the inward facing state and maltose is released in the cytosol. In this model, MalE facilitates the pairing of MalK and the ATP hydrolysis step. *B*, in the proposed new model, ATP alone triggers the outward facing conformation. The outward facing transporter binds unliganded MalE with a high affinity (K_d = ~50–80 nM). Maltose then binds to the MalE-MalFGK$_2$ assembly (K_d = ~120 μM). Upon ATP hydrolysis, the transporter returns to the inward facing conformation, and maltose is released in the cytosol. In this model, MalE stimulates the return of the transporter to the inward facing conformation. If ATP hydrolysis does not take place immediately, or if maltose is present in excess, MalE acquires its closed liganded conformation and dissociates from the transporter (negative autoregulation).

us to propose a new model (Fig. 1*B* and legend for details about the binding affinities).

Here, we further investigate the effect of MalE, maltose, and ATP on the conformation of MalFGK$_2$. Indeed, an important and central question is the mechanism leading to the outward facing conformation. The transition depends on MalE and maltose in the former model, but not in the newer model. Using cross-linking, co-sedimentation analysis, native gels, and fluorescence assays, we show that MalE and closed liganded MalE do not facilitate the closure of MalK dimer, nor the transition of MalFG to the outward facing state. Instead, we find that ATP alone is sufficient. Because MalE does not facilitate the binding of ATP to the transporter (16, 17), nor the outward facing conformation, the results imply that MalE must stimulate a step occurring during the return of the transporter to the inward facing state.

EXPERIMENTAL PROCEDURES

Reagents—The detergent *n*-dodecyl-β-D-maltoside (DDM) was purchased from Anatrace. The lipids 1,2-dioleoyl-*sn*-glycero-3-phosphocholine and 1,2-dioleoyl-*sn*-glycero-3-phospho-(1′-*rac*-glycerol) were purchased from Avanti Polar Lipids. Superdex 200 10/300 GL, Resource 15Q, Sephadex G-25, and Ni^{2+}-NTA chelating Sepharose columns were obtained from GE Healthcare. BioBeads were purchased from Bio-Rad. *N*-(1-Pyrene)-maleimide was obtained from AnaSpec. All other chemicals, including bis-maleimidoethane (BMOE) and *N*-ethylmaleimide, were obtained from Sigma. MalE and His-tagged MalFGK$_2$ were purified as previously described (16), using *Escherichia coli* BL21 (DE3) carrying plasmids pBAD33-MalE or pBAD22-MalFGK$_{his}$.

Reconstitution of MalFGK$_2$ in Nanodiscs and Proteoliposomes—The membrane scaffold protein MSP1D1 was obtained from the Sligar laboratory (18). The lipids 1,2-dioleoyl-*sn*-glycero-3-phosphocholine and 1,2-dioleoyl-*sn*-glycero-3-phospho-(1′-*rac*-glycerol) were mixed at a ratio of 7:3, dissolved in chloroform, and dried under a steam of nitrogen. The lipids were resuspended in TSG buffer (50 mM Tris-HCl, pH 8.0, 100 mM NaCl, 10% glycerol) containing 0.2% DDM. The MalFGK$_2$ complex, the membrane scaffold proteins, and the solubilized lipids were mixed together at a protein:MSP:lipid ratio of 1:3:60 in TSG buffer containing 0.08% DDM. Detergent was removed with BioBeads (one-third volume) and gentle shaking (overnight, 4 °C). BioBeads were removed by sedimentation, and the resulting nanodiscs were purified through Superdex 200 10/30 gel filtration equilibrated in TSG buffer. Proteoliposomes were prepared at a protein:lipid ratio of 1:2000 in TSG buffer containing 0.08% DDM. Detergent was removed using BioBeads as for nanodiscs reconstitution. The proteoliposomes were harvested by centrifugation (100,000 × *g*, 1h, 4 °C) and resuspended in 20 mM Tris-HCl, pH 8.0. The orientation of the complex reconstituted in proteoliposomes was determined by the labeling of residue MalF$_{T177C}$ (in background MalK$_{C40S}$) with 5-iodoacetamide fluorescein (5-IAF). Proteolipsomes (2 μM) were incubated with 5-IAF (10 μM) in 20 mM Tris-HCl, pH 8.0, 1 mM $MgCl_2$ supplemented with or without 1% DDM. The reaction was stopped with DTT (2 mM), and unreacted 5-IAF was removed by gel filtration (Sephadex G-25). Proteoliposomes were extruded through a 100-nm polycarbonate filter before use.

Maltose Transport Assay—Proteoliposomes were reconstituted in R buffer (50 mM sodium phosphate, pH 6.5, 1 mM $MgCl_2$, 5 mM ATP). The transport reaction was carried out with 10 μM MalE, 0.5 μM MalFGK$_2$, and 20 μM [^{14}C]maltose (57 μCi/μmol). At the indicated time, samples (50 μl) were removed and diluted into 1 ml of ice-cold 50 mM sodium phosphate buffer containing 10 mM maltose followed by filtration through a 0.22-μm nitrocellulose Millipore filter and scintillation counting. The number of cpm were converted into nmol using known amounts of [^{14}C]maltose.

Cysteine Cross-linking Experiments—Cross-linking reactions were performed in 50 mM Tris-HCl, pH 8.0, 10 mM $MgCl_2$ containing 0.5 μM MalFGK$_2$ proteoliposomes mixed with 1 mM ATP, 10 μM MalE, and 1 mM maltose as indicated. The samples were incubated with 50 μM BMOE (10 min at room temperature) and then treated with *N*-ethylmaleimide (5 mM) before analysis by SDS-PAGE.

Fluorescence Labeling and Spectroscopy—The dye *N*-(1-pyrene)-maleimide was used to label the MalFGK$_2$ cysteine mutants. Briefly, the purified MalFGK$_2$ complex was incubated

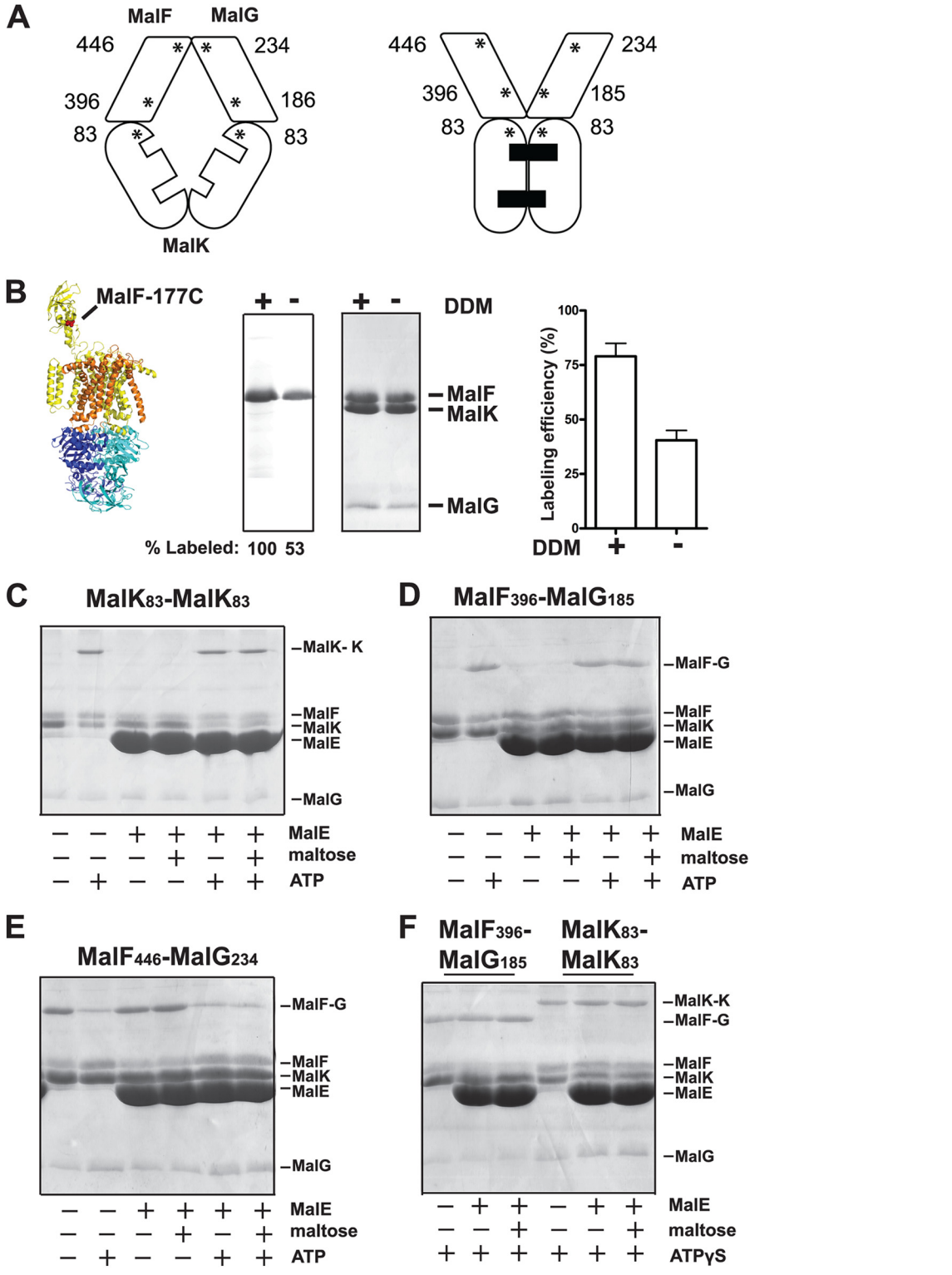

FIGURE 2. **ATP triggers the transporter outward facing conformation.** *A*, the *asterisks* indicate the location of the cysteine residues introduced in MalF, MalG, and MalK and their relative positions in the inward and outward facing conformations. *B*, orientation of the MalFGK$_2$ complex in proteoliposomes. The labeling efficiency of residue MalF$_{T177C}$ (in mutant background MalK$_{C40S}$) was assayed using the membrane-impermeable reagent 5-IAF in the presence or absence of DDM. The samples were analyzed by 15% SDS-PAGE followed by fluorescence scanning (*left panel*) or Coomassie Blue staining (*right panel*). The fluorescence of MalF$_{T177C}$ when labeled in the presence of DDM was normalized to 100%. The labeling efficiency of MalF$_{T177C}$ was determined by absorbance spectroscopy (498 nm), using an extinction co-efficient of 75, 500 cm^{-1} M^{-1}. *C–E*, the indicated transporters reconstituted in proteoliposomes were incubated with the homobifunctional cross-linker BMOE (50 μM) in the indicated conditions. The samples were treated with *N*-ethylmaleimide (5 mM) prior to analysis by 15% SDS-PAGE and Coomassie Blue staining. *F*, cross-linking results for the pairs MalF$_{396}$/MalG$_{185}$ and MalF$_{446}$/MalG$_{234}$ in the presence of ATPγS.

TABLE 1

The affinity of MalE for the transporter in nanodiscs determined by fluorescence quenching assay as previously described (16)

Vi, vanadate; Nu, nucleotide; NA, not applicable.

Transporter	Affinity for MalE[a]				
	ATP + Vi	ATP + BMOE	No Nu	No Nu + BMOE	No Nu + maltose
			μM		
Wild type	0.079 ± 0.009	1.41 ± 0.07	7.14 ± 1.13	5.71 ± 1.06	45.24 ± 19.32
$MalK_{83}$-$MalK_{83}$	0.046 ± 0.007	0.057 ± 0.006	6.93 ± 1.21	5.12 ± 0.74	NA
$MalF_{396}$-$MalG_{185}$	0.064 ± 0.011	0.073 ± 0.010	6.43 ± 1.42	4.32 ± 0.94	NA
$MalF_{446}$-$MalG_{234}$	0.085 ± 0.008	1.18 ± 0.13[b]	7.17 ± 1.65	13.73 ± 3.54	>45[c]

[a] The data are derived from three independent measurements, and the fit is using a one-site binding equation.
[b] The measurement was performed in the presence of Vi.
[c] The measurement was performed using cross-linked $MalF_{446}$-$MalG_{234}$.

with 0.5 mM DTT (30 min on ice) and passed through a G25 column. The labeling reaction was then performed by mixing $MalFGK_2$ and *N*-(1-pyrene)-maleimide at a molar ratio of 1:10 in TSG buffer containing 0.01% DDM and 1 mM TCEP for 2 h at room temperature. The unreacted *N*-(1-pyrene)-maleimide was removed by Superdex 200 10/30 gel filtration. The purified and labeled complex was reconstituted in proteoliposomes as described above. The labeling efficiency was determined by absorbance spectroscopy (343 nm) using an extinction co-efficient of 40,000 cm^{-1} M^{-1}. A typical ratio was between 1.2 and 1.4. Because there are two cysteine substitutions per $MalFGK_2$ variant, this is equal to ~60–70% labeling efficiency. The pyrene-labeled $MalFGK_2$ variants retained ~80% ATPase activity and 70% transport activity of wild type $MalFGK_2$ (see Table 2). The fluorescent measurements were carried out at 25 °C in FL buffer (50 mM Tris-HCl, pH 8.0, 5 mM $MgCl_2$) on a Cary Eclipse spectrofluorometer. The fluorescence spectrums were recorded from 365 to 520 nm with excitation wavelength at 345 nm (5-nm slide width). The binding of MalE to $MalFGK_2$ was measured by fluorescence quenching assay, using MalE-31C labeled with the maleimide derivative ATTO-655 (Atto-Tech), as previously described (16). The fluorescent measurements were carried out at 25 °C in FL buffer.

Other Methods—The transporter ATPase activity was determined by measuring the release of inorganic phosphate using photo colorimetric method (16). Linear gradient native gel electrophoresis, sedimentation assay, and protein iodination were performed as described (16, 19).

RESULTS

ATP Controls the Outward Facing Conformation of the Transporter—Cysteine residues were introduced at diagnostic positions on MalK, MalF, and MalG, so that sulfhydryl-based cross-linking methods could be employed to monitor the conformation of the transporter in the lipid bilayer (Fig. 2*A*). The cysteine residues were introduced into a complex mutated at the endogenous Cys-40 of MalK because this position naturally reacts with maleimide reagents (data not shown). According to the crystallographic data (8, 9), the distance between the periplasmic positions $MalF_{446}$/$MalG_{234}$ increases from ~9 to ~18 Å during the conformational transition from the inward facing state to the outward facing state. Meanwhile, the distance between the cytosolic positions $MalK_{83}$/$MalK_{83}$ and $MalF_{396}$/$MalG_{185}$ decreases from ~ 21 to ~8 Å. We thus employed the homobifunctional cross-linker BMOE with a spacer arm of 8 Å to monitor these conformational changes (Fig. 2).

We note that the C-terminal tail of MalG in the crystal structure is located near the MalK dimer interface and may potentially interfere with the formation of the cross-link $MalK_{83}$/$MalK_{83}$. However, as reported by others, an efficient ATP-dependent cross-linking occurs with this pair (and also with $MalK_{85}$/$MalK_{85}$), showing that the C-terminal tail of MalG is sufficiently mobile in solution to allow cross-link formation (20, 21). We also considered the possibility that $MalFGK_2$ becomes inaccessible to MalE when the transporter is reconstituted in liposomes. This was ruled out because (i) the transporter was functional (Table 1), and its activity was dependent on MalE and maltose, (ii) the sedimentation of MalE with the proteoliposome was dependent on $MalFGK_2$ and nucleotides (Fig. 3, *A* and *C*), and (iii) the thiol-reactive membrane-impermeable reagent 5-IAF labeled the periplasmic side of the complex with at least 50% efficiency (Fig. 2*B*).

We then probed what the transporter conformation is in the membrane. In the absence of ligands (apo state), there was only a little cross-link formation with the pairs $MalK_{83}$/$MalK_{83}$ and $MalF_{396}$/$MalG_{185}$ (pairs located in the cytosolic side of the membrane), whereas cross-links readily formed with the pair $MalF_{446}$/$MalG_{234}$ (located on the periplasmic side) (Fig. 2, *C–E*). These results were expected because the transporter resides naturally in the inward facing state in the absence of ligands (8). In the presence of ATP, however, a predominant cross-link appeared with the pairs $MalK_{83}$/$MalK_{83}$ and $MalF_{396}$/$MalG_{185}$, whereas the cross-link of $MalF_{446}$/$MalG_{234}$ was decreased by ~90%, as determined by densitometry analysis (data not shown). The binding of ATP, and not its hydrolysis, was responsible for this conformational change because ATPγS produced the same effect (Fig. 2*F*). Strikingly, the addition of MalE with or without maltose did not cause any differences in the cross-linking efficiencies (Fig. 2, *C–F*). Together, these data provided strong preliminary evidence that ATP on its own controls the transition of the transporter from inward to outward facing state.

ATP Controls the Binding of MalE to the Transporter—We reported recently that MalE binds with nanomolar affinity to the outward facing transporter (16). Because ATP alone appears sufficient for the transition to the outward facing conformation, we hypothesized that ATP alone should also control the binding of MalE to the transporter. Accordingly, the stabilization of $MalFGK_2$ in the outward facing state with ATP plus vanadate allowed an efficient co-sedimentation of MalE with the transporter (Fig. 3*A*, *lanes 2*). In the absence of vanadate, the binding of MalE was weak because the transporter hydrolyzes

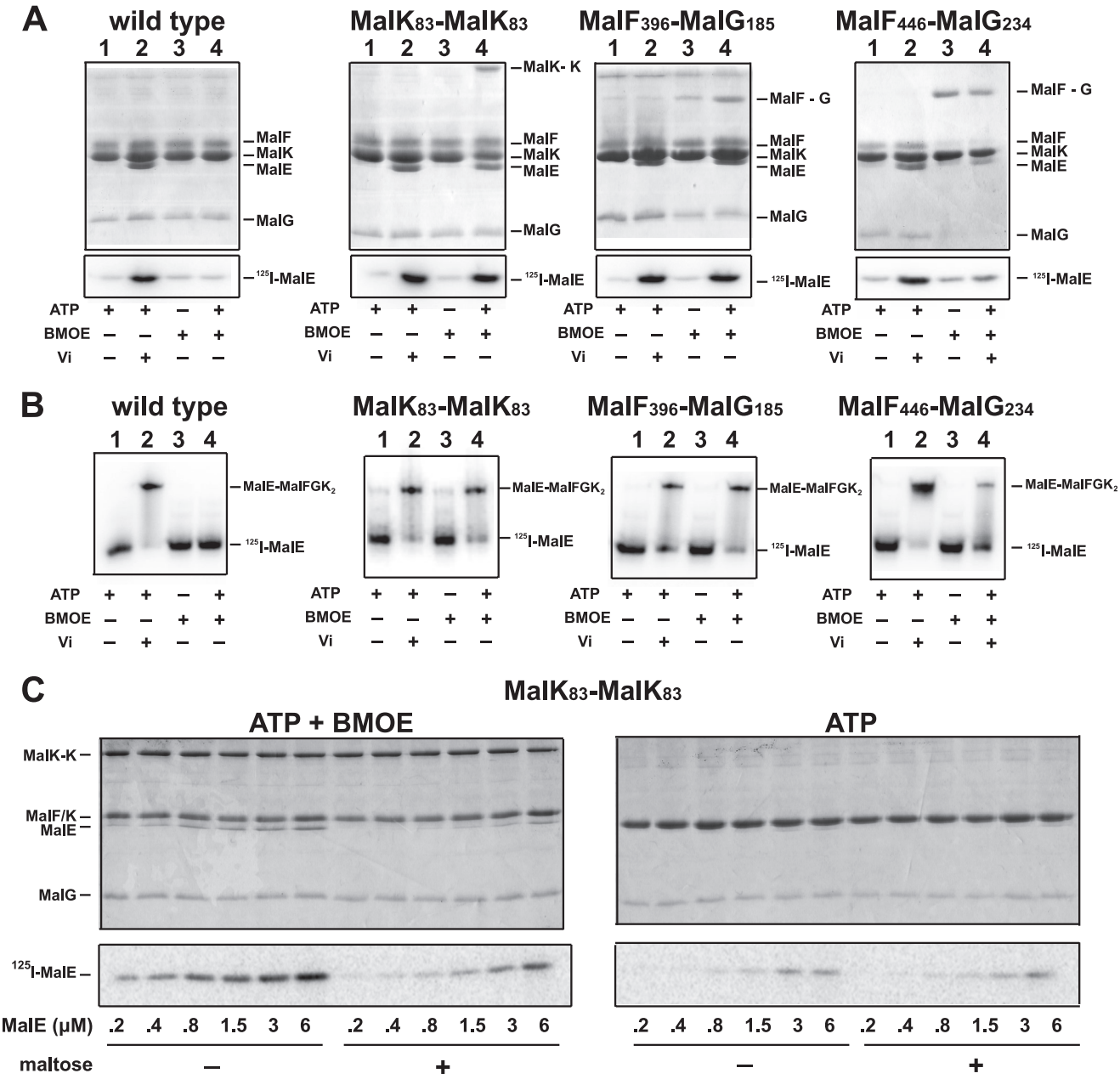

FIGURE 3. **ATP controls the binding of MalE to the transporter.** *A*, the binding of MalE to MalFGK$_2$ in proteoliposomes was analyzed by co-sedimentation assay. [^{125}I]MalE (~10,000 cpm, 10 μM) was incubated with MalFGK$_2$ proteoliposomes (2 μM) in the presence of ATP, vanadate, and BMOE as indicated (room temperature, 10 min). The samples were diluted 25-fold in 20 mM Tris-HCl, pH 8.0, before ultracentrifugation (100,000 × *g*, 1 h). The fraction of MalE bound to MalFGK$_2$ was analyzed by 15% SDS-PAGE followed by Coomassie Blue staining (*top panels*) or autoradiography (*bottom panels*). *B*, the binding of [^{125}I]MalE to MalFGK$_2$ in nanodiscs was analyzed by native gel electrophoresis. [^{125}I]MalE (~5,000 cpm, 0.5 μM) was incubated with MalFGK$_2$ nanodiscs (1 μM) in the presence of ATP, vanadate, and BMOE as indicated (room temperature, 10 min). The samples were analyzed by native gel electrophoresis and autoradiography. *C*, maltose promotes the dissociation of MalE when MalFGK$_2$ is stabilized in the outward facing state. The binding of MalE to MalFGK$_2$ in proteoliposomes was analyzed by sedimentation assay. The indicated amount of [^{125}I]MalE was incubated with MalFGK$_2$ (pair MalK$_{83}$-MalK$_{83}$) in proteoliposomes in the presence of ATP or ATP and BMOE (room temperature, 10 min). The samples were diluted 25-fold in 20 mM Tris-HCl, pH 8, with or without 1 mM maltose. The fraction of MalE bound to MalFGK$_2$ was isolated by ultracentrifugation (100,000 × *g*, 1 h). The amount of bound MalE was analyzed by 12% SDS-PAGE followed by Coomassie Blue staining (*top panels*) or autoradiography (*bottom panels*). Note that MalF and MalK are migrating at the same position on 12% SDS-PAGE.

ATP and returns to the inward facing conformation, which has no affinity for MalE. Accordingly, when the mutants MalK$_{83}$/MalK$_{83}$ and MalF$_{396}$/MalG$_{185}$ were treated with ATP plus BMOE to stabilize the transporter in the outward facing state, the binding of MalE was as efficient as with ATP plus vanadate (Fig. 3*A*, compare *lanes 2* with *lanes 4*). In contrast, when the transporter was locked in the inward facing state with the pair MalF$_{446}$/MalG$_{234}$, the binding of MalE was at background levels, even in the presence of ATP and vanadate (Fig. 3*A*, *right panel*, *lane 4*). The results therefore confirm that ATP controls the transition from inward to outward facing state, which in turn controls the binding of MalE to the transporter.

We next employed a fluorescence-based assay to determine the binding affinity of MalE to MalFGK$_2$ in the inward and outward facing states. We reconstituted the transporter in

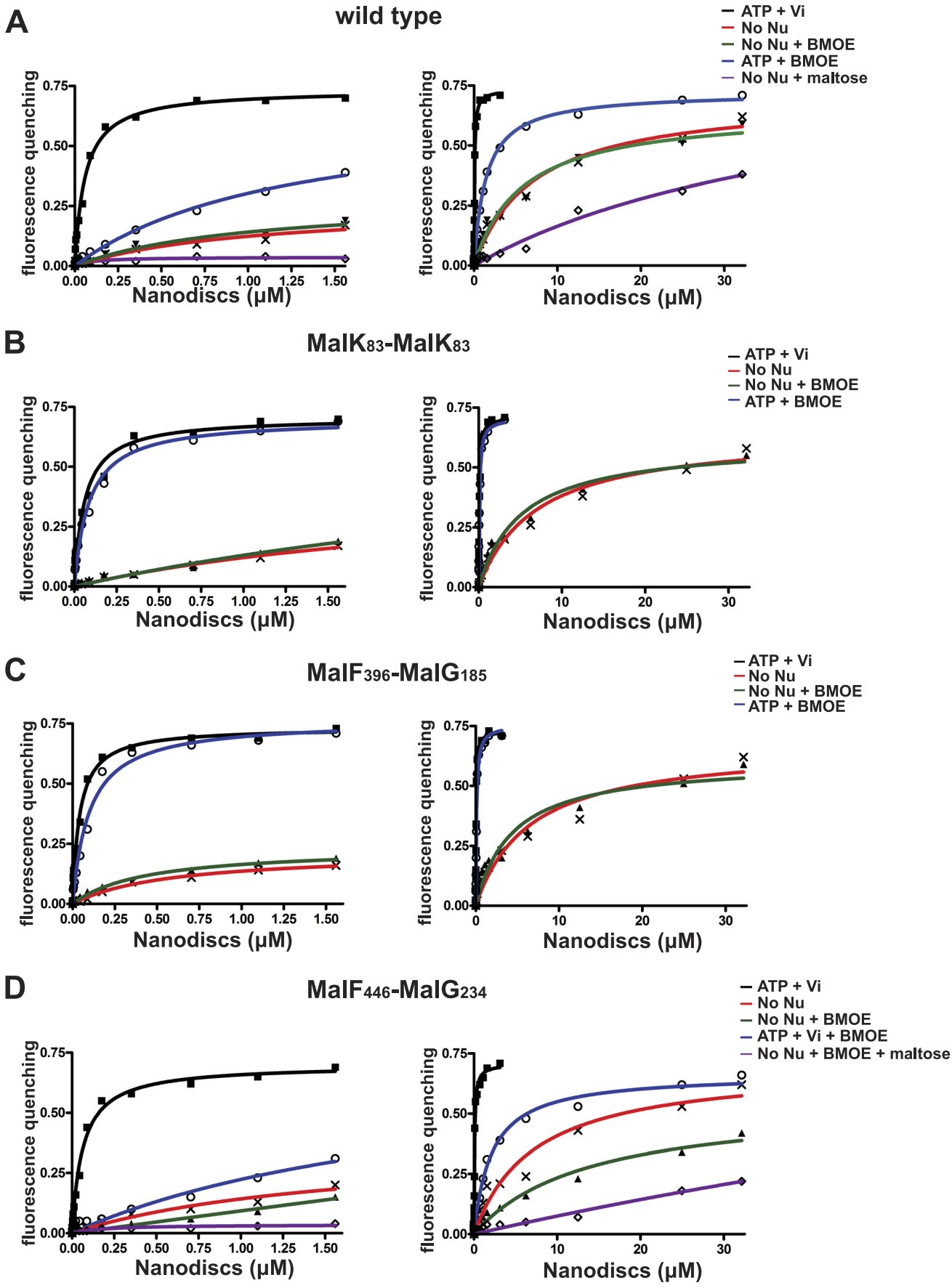
A
wild type
ATP + Vi
No Nu
No Nu + BMOE
ATP + BMOE
No Nu + maltose
fluorescence quenching
Nanodiscs (μM)
B
MalK83-MalK83
ATP + Vi
No Nu
No Nu + BMOE
ATP + BMOE
C
MalF396-MalG185
ATP + Vi
No Nu
No Nu + BMOE
ATP + BMOE
D
MalF446-MalG234
ATP + Vi
No Nu
No Nu + BMOE
ATP + Vi + BMOE
No Nu + BMOE + maltose

TABLE 2
ATPase activity of the pyrene-labeled transporters reconstituted in proteoliposomes

Transporter	ATPase activity	Transport activity		
	−MalE and maltose	+MalE and maltose	−MalE	+MalE
	nmol/min/mg		*nmol/min/mg*	
Wild type	11 ± 4	892 ± 91	0–0.1	2.3 ± 0.4
$MalK_{83}$-$MalK_{83}$	9 ± 2	734 ± 65	0–0.1	1.8 ± 0.3
$MalF_{396}$-$MalG_{185}$	12 ± 3	792 ± 84	0–0.1	1.7 ± 0.4
$MalF_{446}$-$MalG_{234}$	7 ± 2	704 ± 73	0–0.1	1.5 ± 0.2

nanodisc because the system is well suited for spectroscopic analysis (22). First, we confirmed on native gel that MalE binds to the transporter with the same characteristics in nanodiscs as in proteoliposomes (Fig. 3, compare *B* with *A*; ATP dependence). We then titrated the fluorescent-labeled MalE with an increasing amount of transporter (Fig. 4). The data showed that MalE binds with a high affinity (K_d = ~50–80 nM) only when the transporter is stabilized in the outward facing conformation with ATP-vanadate or ATP-BMOE (binding data and standard deviations reported in Table 1). In contrast, in the absence of nucleotides, the binding affinity of MalE for the transporter was ~7 μM and increased furthermore to ~45 μM when MalE was liganded with maltose (Table 1 and Fig. 3*C*). Because the transporter might spontaneously acquire its outward facing conformation even in the absence of ATP, the affinity of liganded MalE to the inward facing state may in fact be lower than 45 μM. Indeed, the interaction of maltose-bound MalE was virtually null when the transporter was stabilized in the inward facing state using the cysteine pair $MalF_{446}$/$MalG_{234}$ (Fig. 4*D*). The reaction was not saturable, and therefore the affinity could not be determined, in agreement with earlier binding assays in proteoliposomes (23). We concluded that ATP controls the transporter outward facing conformation and thereby controls the high affinity binding of MalE to the transporter.

MalE Does Not Facilitate the Transition to the Outward Facing Conformation—As an additional way to probe the transporter conformational state and to explore the transition kinetics, we employed the fluorescent dye *N*-(1-pyrene) maleimide. When attached to a protein thiol, the dye produces two distinct emission peaks at 375 and 395 nm. When two pyrene-thiols interact within 6–10 Å distance, they form excited state dimers (excimers) that emit at longer wavelengths than the lone excited fluorophore (24, 25). The transporter labeled with the pyrene probe at the cysteine positions described above retained ~80% ATPase activity and 70–80% maltose transport activity as compared with the wild type complex (Table 2). The fluorescence spectra were recorded between 365 and 520 nm to monitor the conformational changes in the presence of ATP, MalE, and maltose (Fig. 5, *red traces*), compared with without ligands (*black traces*). With the pairs $MalK_{83}$/$MalK_{83}$ and $MalF_{396}$/$MalG_{185}$, which monitor the conformational changes on the cytosolic side of the membrane, ATP decreased the monomeric emissions but increased the excimer emissions (Fig. 5, *A* and *B*). The reverse was observed with the pair $MalF_{446}$/$MalG_{234}$. This was expected because the pair monitors the conformational change on the opposite side of the membrane (Fig. 5*C*). In contrast, MalE and maltose had no effect on the monomeric and excimer emissions, in agreement with the conclusion that ATP alone supports the outward facing conformation of the transporter. Furthermore, we observed that MalE and maltose had no effect on the kinetics of the conformational transition (Fig. 6). These time-resolved experiments showed that liganded MalE is unable to modify the kinetics of MalK closure, even though we employed a cysteine pair that produced the highest fluorescence signal difference (*i.e.*, $MalK_{83}$/$MalK_{83}$). We therefore conclude that MalE is not required, nor does it facilitate the closure of the nucleotide-binding domain in the intact and functional maltose ABC transporter.

DISCUSSION

We report that ATP alone is sufficient for the closure of the MalK interface and for the conversion of MalFG to the outward facing conformation. This conclusion is based on cysteine cross-links and pyrene-based fluorescence of probes placed at diagnostic positions on the transporter. The cysteine substitutions and the pyrene label affect modestly the ATPase activity of the transporter, and do not affect its capacity to import maltose (*i.e.*, 70–80% activity of the wild type; Table 2). The conclusion we reach is in fact not surprising but rather in agreement with other studies reporting that ATP drives the dimerization of MalK in the membrane or in solution (26–28). The conclusion is also consistent with the x-ray structures that showed the rigid body rotation of MalFG upon closure of MalK (8). That ATP alone regulates the conformation of the transporter has also been reported for other type I and type II importers (ModBC and BtuCD, respectively), as well as for ABC exporters (7, 29–32).

Our results, however, disagree with the accepted notion that closed liganded MalE facilitates the closure of the MalK dimer. This mechanism was proposed (and perhaps intuitively accepted) because a rapid ATP hydrolysis activity occurs only in the presence of MalE and maltose. To the best of our knowledge, this model has been directly tested by EPR spectroscopy only (14). Why the study concluded that MalK closure strictly depends on MalE is puzzling. The spin label reduced the MalK ATPase activity by 2-fold (from 2,100 to 1,150 nmol/min/mg), yet the transporter was still active. The spin labels were, however, placed at two different positions on the same MalK subunit, giving rise to four different possible ways of spin interactions. Most importantly, the EPR distance measurements were performed in detergent solution, whereas the transporter ATPase is ~100-fold higher than in the membrane and poorly dependent on MalE and maltose (16). The sensitivity of EPR in the membrane environment is indeed problematic because of

FIGURE 4. **Equilibrium titration of MalE binding to MalFGK$_2$ in nanodiscs.** The $MalFGK_2$ complex in nanodiscs was incubated with ATP (1 mM), BMOE (50 μM), and vanadate (10 μM) as indicated (10 min at room temperature). The nanodiscs were repurified on a desalting G25 column before fluorescence quenching assay using ATTO-655-labeled MalE (20 nM). Three independent measurements were performed, and the data points were fitted to a one-site binding equation (mean and standard deviation results are presented in Table 1). *A*, $MalFGK_2$ wild type. *B*, $MalFGK_2$ with mutations $MalK_{S83C}$/$MalK_{C40S}$ ($MalK_{83}$-$MalK_{83}$). *C*, $MalFGK_2$ with mutations $MalF_{P396C}$/$MalG_{D185C}$/$MalK_{C40S}$ ($MalF_{396}$-$MalG_{185}$). *D*, $MalFGK_2$ with mutations $MalF_{L446C}$/$MalG_{S234C}$/$MalK_{C40S}$ ($MalF_{446}$-$MalG_{234}$). The *left* and *right panels* are the same curves but fitted to a different *x* axis.

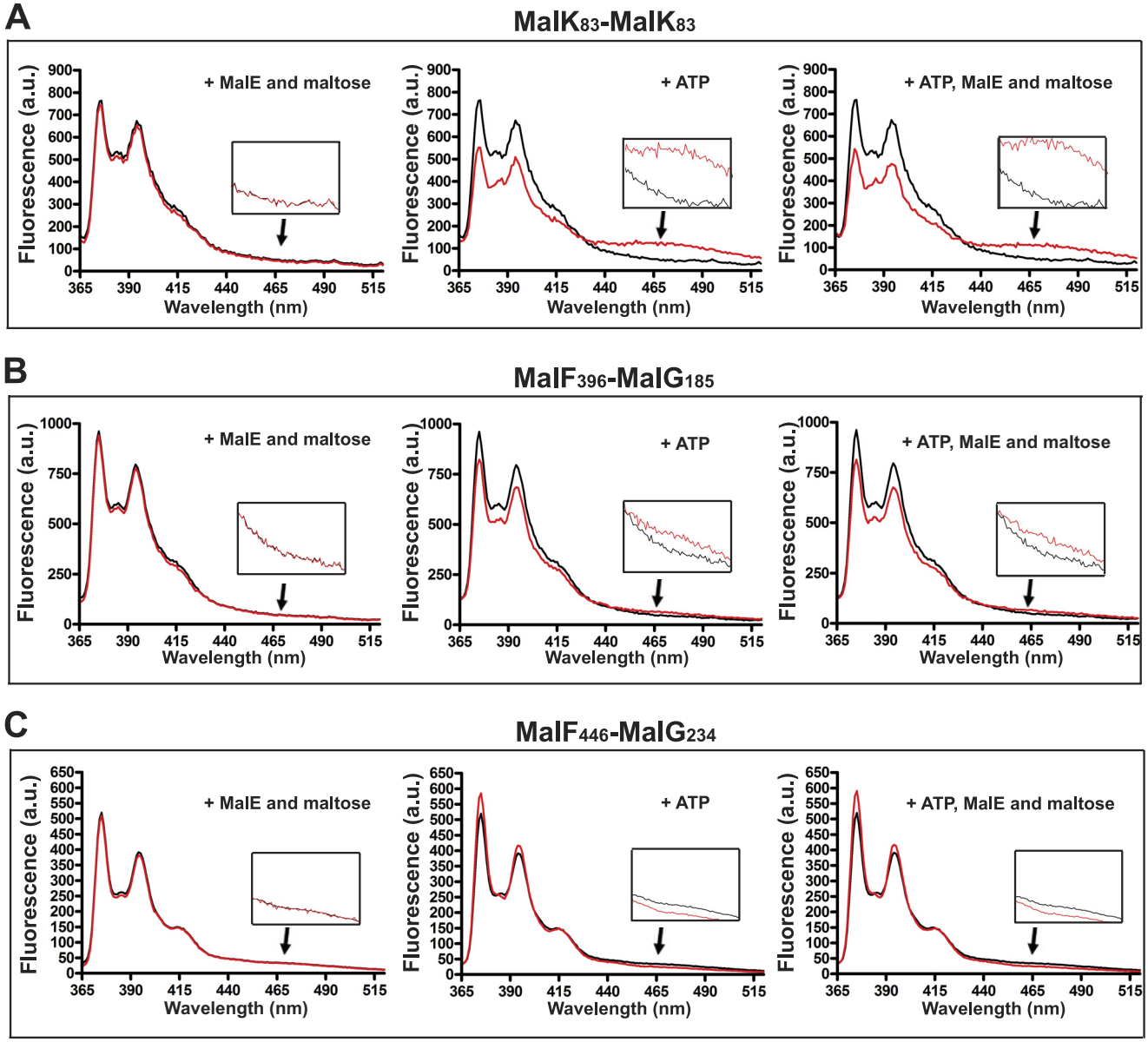

FIGURE 5. **Neither MalE nor maltose facilitates the transition to the outward facing state.** The steady state fluorescence emission spectra of pyrene-labeled MalFGK$_2$ recorded in the absence (*black traces*) or presence of ATP, MalE, and maltose (*red traces*) using the following pyrene-labeled MalFGK$_2$ transporters: MalK$_{83}$/MalK$_{83}$ (*A*), MalF$_{396}$/MalG$_{185}$ (*B*), and MalF$_{446}$/MalG$_{234}$ (*C*). The fluorescence spectra were recorded from 365 to 520 nm with excitation wavelength at 345 nm. The fluorescence spectra recorded around 465 nm are magnified in the *insets*.

the large spin decay inherent to intermolecular dipolar interactions (33), and accordingly, the authors could not report the interspin distances with the transporter reconstituted in liposomes. Nevertheless, this pioneering work showed that ATP is essential for the pairing of MalK, and this conclusion is consistent with our results.

Our results also contrast with the interpretation of the crystal structure that captured closed liganded MalE with the transporter in a semi-closed conformation (15). It was concluded that closed liganded MalE binds to MalFG and induces the preclosure of MalK and thus ATP hydrolysis. Our pyrene-based fluorescence experiments rather show that the kinetics of MalK pairing is the same, whether MalE and maltose are present or not (Fig. 5). In addition, we find that the binding of closed liganded MalE to the inward facing transporter is quasi-null in solution ($K_d > 45$ μM; Table 1). In contrast, the binding of MalE to the outward facing transporter occurs with nanomolar affinity ($K_d = \sim 60$ nM; Table 1). Clearly, a far more dominant interaction is taking place between ATP-bound outward facing MalFGK$_2$ and unliganded open state MalE. Given the high concentration of ATP in the cytosol (~1 mM), we think this mode of interaction represents the resting state of the transporter. This view is supported by an *in vivo* cross-linking analysis, which reported that MalE is bound to the transporter even in the absence of maltose (34). This view is also consistent with our conclusion that transporter-bound MalE forms a receptor for maltose (16). In contrast, a model involving the low affinity interaction between closed liganded MalE and MalFGK$_2$ ($K_d >$ 45 μM), as a way to deliver the sugar and activate the transporter, seems unsustainable because the concentration of

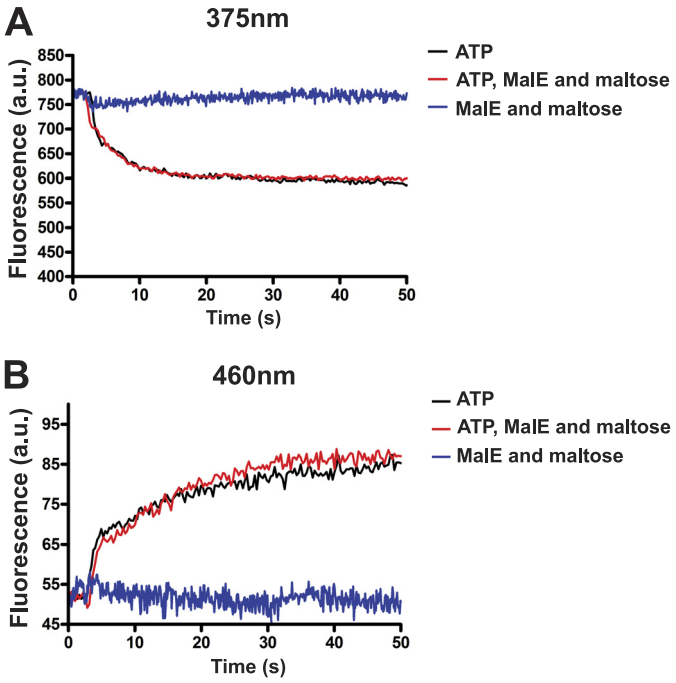

FIGURE 6. **Transition kinetics toward the outward facing conformation.** The time course fluorescence emission spectra for the pair MalK$_{83}$/MalK$_{83}$ were monitored after the addition of ATP, MalE, and maltose as indicated. The spectra were recorded at 375 nm to monitor pyrene monomers (*A*) and 460 nm to monitor exited state dimers (*B*). The fluorescence is expressed in arbitrary units as in Fig. 4.

periplasmic MalE decreases further as the environmental maltose concentration decreases.

An obvious question raised by this work is how MalE stimulates the MalK ATPase. The co-crystal of closed liganded MalE with MalFGK$_2$ has led to the proposal that MalE lowers the energy barrier for ATP hydrolysis (15). However, it cannot be excluded that the binding of MalE to the outward facing transporter instead stimulates the release of ADP and/or Pi and thus the ATP turnover rate (and furthermore in the presence of maltose). Earlier studies suggested that ATP product release may coincide with the reorientation of MalFGK$_2$ to the inward facing conformation (14). For the mammalian P-glycoprotein, it was proposed that phosphate release is coupled to transport (35). Further work should therefore address what is the rate-limiting step during maltose transport. Our current work shows that the affinity of the transporter for ATP is not increased with MalE (16) and that ATP alone is sufficient to convert the transporter to the outward facing conformation. Together, these results imply that MalE must stimulate a step that occurs when the transporter returns to the inward facing conformation. This conclusion is compatible with the autoregulation model presented in Fig. 1*B*.

REFERENCES

1. Rees, D. C., Johnson, E., and Lewinson, O. (2009) ABC transporters. The power to change. *Nat. Rev. Mol. Cell Biol.* **10,** 218–227
2. Davidson, A. L., Dassa, E., Orelle, C., and Chen, J. (2008) Structure, function, and evolution of bacterial ATP-binding cassette systems. *Microbiol. Mol. Biol. Rev.* **72,** 317–364
3. Shilton, B. H. (2008) The dynamics of the MBP-MalFGK$_2$ interaction. A prototype for binding protein dependent ABC-transporter systems. *Biochim. Biophys. Acta* **1778,** 1772–1780
4. Bordignon, E., Grote, M., and Schneider, E. (2010) The maltose ATP-binding cassette transporter in the 21st century. Towards a structural dynamic perspective on its mode of action. *Mol. Microbiol.* **77,** 1354–1366
5. Procko, E., O'Mara, M. L., Bennett, W. F., Tieleman, D. P., and Gaudet, R. (2009) The mechanism of ABC transporters. General lessons from structural and functional studies of an antigenic peptide transporter. *FASEB J.* **23,** 1287–1302
6. Oldham, M. L., and Chen, J. (2011) Snapshots of the maltose transporter during ATP hydrolysis. *Proc. Natl. Acad. Sci. U.S.A.* **108,** 15152–15156
7. Hollenstein, K., Dawson, R. J., and Locher, K. P. (2007) Structure and mechanism of ABC transporter proteins. *Curr. Opin. Struct. Biol.* **17,** 412–418
8. Khare, D., Oldham, M. L., Orelle, C., Davidson, A. L., and Chen, J. (2009) Alternating access in maltose transporter mediated by rigid-body rotations. *Mol. Cell.* **33,** 528–536
9. Oldham, M. L., Khare, D., Quiocho, F. A., Davidson, A. L., and Chen, J. (2007) Crystal structure of a catalytic intermediate of the maltose transporter. *Nature* **450,** 515–521
10. Spurlino, J. C., Lu, G. Y., and Quiocho, F. A. (1991) The 2.3-A resolution structure of the maltose- or maltodextrin-binding protein, a primary receptor of bacterial active transport and chemotaxis. *J. Biol. Chem.* **266,** 5202–5219
11. Sharff, A. J., Rodseth, L. E., Spurlino, J. C., and Quiocho, F. A. (1992) Crystallographic evidence of a large ligand-induced hinge-twist motion between the two domains of the maltodextrin binding protein involved in active transport and chemotaxis. *Biochemistry* **31,** 10657–10663
12. Davidson, A. L., Shuman, H. A., and Nikaido, H. (1992) Mechanism of maltose transport in *Escherichia coli*. Transmembrane signaling by periplasmic binding proteins. *Proc. Natl. Acad. Sci. U.S.A.* **89,** 2360–2364
13. Davidson, A. L. (2002) Mechanism of coupling of transport to hydrolysis in bacterial ATP-binding cassette transporters. *J. Bacteriol.* **184,** 1225–1233
14. Orelle, C., Ayvaz, T., Everly, R. M., Klug, C. S., and Davidson, A. L. (2008) Both maltose-binding protein and ATP are required for nucleotide-binding domain closure in the intact maltose ABC transporter. *Proc. Natl. Acad. Sci. U.S.A.* **105,** 12837–12842
15. Oldham, M. L., and Chen, J. (2011) Crystal structure of the maltose transporter in a pretranslocation intermediate state. *Science* **332,** 1202–1205
16. Bao, H., and Duong, F. (2012) Discovery of an auto-regulation mechanism for the maltose ABC transporter MalFGK2. *PLoS One* **7,** e34836
17. Reich-Slotky, R., Panagiotidis, C., Reyes, M., and Shuman, H. A. (2000) The detergent-soluble maltose transporter is activated by maltose binding protein and verapamil. *J. Bacteriol.* **182,** 993–1000
18. Denisov, I. G., Grinkova, Y. V., Lazarides, A. A., and Sligar, S. G. (2004) Directed self-assembly of monodisperse phospholipid bilayer Nanodiscs with controlled size. *J. Am. Chem. Soc.* **126,** 3477–3487
19. Dalal, K., and Duong, F. (2010) Reconstitution of the SecY translocon in nanodiscs. *Methods Mol. Biol.* **619,** 145–156
20. Daus, M. L., Grote, M., Müller, P., Doebber, M., Herrmann, A., Steinhoff, H. J., Dassa, E., and Schneider, E. (2007) ATP-driven MalK dimer closure and reopening and conformational changes of the "EAA" motifs are crucial for function of the maltose ATP-binding cassette transporter (MalFGK$_2$). *J. Biol. Chem.* **282,** 22387–22396
21. Grote, M., Bordignon, E., Polyhach, Y., Jeschke, G., Steinhoff, H. J., and Schneider, E. (2008) A comparative electron paramagnetic resonance study of the nucleotide-binding domains' catalytic cycle in the assembled maltose ATP-binding cassette importer. *Biophys. J.* **95,** 2924–2938
22. Bayburt, T. H., and Sligar, S. G. (2010) Membrane protein assembly into Nanodiscs. *FEBS Lett.* **584,** 1721–1727
23. Austermuhle, M. I., Hall, J. A., Klug, C. S., and Davidson, A. L. (2004) Maltose-binding protein is open in the catalytic transition state for ATP hydrolysis during maltose transport. *J. Biol. Chem.* **279,** 28243–28250
24. Sahoo, D., Narayanaswami, V., Kay, C. M., and Ryan, R. O. (2000) Pyrene excimer fluorescence. A spatially sensitive probe to monitor lipid-induced helical rearrangement of apolipophorin III. *Biochemistry* **39,** 6594–6601
25. Lehrer, S. S. (1995) Pyrene excimer fluorescence as a probe of protein conformational change. *Subcell. Biochem.* **24,** 115–132
26. Hunke, S., Mourez, M., Jehanno, M., Dassa, E., and Schneider, E. (2000) ATP modulates subunit-subunit interactions in an ATP-binding cassette

transporter (MalFGK$_2$) determined by site-directed chemical cross-linking. *J. Biol. Chem.* **275,** 15526–15534
27. Daus, M. L., Grote, M., Müller, P., Doebber, M., Herrmann, A., Steinhoff, H. J., Dassa, E., and Schneider, E. (2007) ATP-driven MalK dimer closure and reopening and conformational changes of the "EAA" motifs are crucial for function of the maltose ATP-binding cassette transporter (MalFGK2). *J. Biol. Chem.* **282,** 22387–22396
28. Smith, P. C., Karpowich, N., Millen, L., Moody, J. E., Rosen, J., Thomas, P. J., and Hunt, J. F. (2002) ATP binding to the motor domain from an ABC transporter drives formation of a nucleotide sandwich dimer. *Mol. Cell* **10,** 139–149
29. Gerber, S., Comellas-Bigler, M., Goetz, B. A., and Locher, K. P. (2008) Structural basis of trans-inhibition in a molybdate/tungstate ABC transporter. *Science* **321,** 246–250
30. Goetz, B. A., Perozo, E., and Locher, K. P. (2009) Distinct gate conformations of the ABC transporter BtuCD revealed by electron spin resonance spectroscopy and chemical cross-linking. *FEBS Lett.* **583,** 266–270
31. Joseph, B., Jeschke, G., Goetz, B. A., Locher, K. P., and Bordignon, E. (2011) Transmembrane gate movements in the type II ATP-binding cassette (ABC) importer BtuCD-F during nucleotide cycle. *J. Biol. Chem.* **286,** 41008–41017
32. Locher, K. P. (2009) Review. Structure and mechanism of ATP-binding cassette transporters. *Philos. Trans. R. Soc. Lond. B Biol. Sci.* **364,** 239–245
33. McHaourab, H. S., Steed, P. R., and Kazmier, K. (2011) Toward the fourth dimension of membrane protein structure. Insight into dynamics from spin-labeling EPR spectroscopy. *Structure* **19,** 1549–1561
34. Daus, M. L., Berendt, S., Wuttge, S., and Schneider, E. (2007) Maltose binding protein (MalE) interacts with periplasmic loops P2 and P1 respectively of the MalFG subunits of the maltose ATP binding cassette transporter (MalFGK$_2$) from *Escherichia coli*/*Salmonella* during the transport cycle. *Mol. Microbiol.* **66,** 1107–1122
35. Urbatsch, I. L., Sankaran, B., Bhagat, S., and Senior, A. E. (1995) Both P-glycoprotein nucleotide-binding sites are catalytically active. *J. Biol. Chem.* **270,** 26956–26961